Which impedance strategy is the most effective for cooperative object manipulation?

Payam Zarafshan
Department of Agro-Technology, Abouraihan Collage, University of Tehran, Tehran, Iran
Reza Larimi
School of Engineering, The University of British Columbia, Kelowna, Canada
S. Ali A. Moosavian
Center of Excellence in Robotics and Control, Advanced Robotics and Automated Systems Lab, Department of Mechanical Engineering, K.N. Toosi University of Technology, Tehran, Iran, and
Bruno Siciliano
PRISMA Lab, Department of Electrical Engineering and Information Technology, University of Naples Federico II, Naples, Italy

Abstract

Purpose – The purpose of this paper is to present a comparison study of cooperative object manipulation control algorithms. To this end, a full comprehensive survey of the existing control algorithms in this field is presented.

Design/methodology/approach – Cooperative manipulation occurs when manipulators are mechanically coupled to the object being manipulated, and the manipulators may not be treated as an isolated system. The most important and basic impedance control (IC) strategies for an assumed cooperative object manipulation task are the Augmented Object Model (AOM) control and the multiple impedance control (MIC) which are found based on the IC, where the former is designed based on the object movement, and the latter is designed based on the whole robot movement. Thus, the basis of these two algorithms are fully studied.

Findings – The results are fully analyzed, and it is practically verified that the MIC algorithm has the better performance. In fact, the results reveal that the MIC system could successfully perform the object manipulation task, as opposed to the AOM controller: for the same controller gains, the MIC strategy showed better performance than the AOM strategy. This means that because there is no control on the robot base with the AOM algorithm, the object manipulation task cannot be satisfactorily performed whenever the desired path is not within the robot work space. On the other hand, with the MIC algorithm, satisfactory object manipulation is achieved for a mobile robotic system in which the robot base, the manipulator endpoints and the manipulated object shall be moved.

Practical implications – A simple conceptual model for cooperative object manipulation is considered, and a suitable setup is designed for practical implementation of the two ICs.

Originality/value – The basis of these two aspects or these two algorithms is fully studied and compared which is the foundation of this paper. For this purpose, a case study is considered, in which a space free-flying robotic system, which contains two 2-degrees of freedom planar cooperative manipulators, is simulated to manipulate an object using the above control strategies. The system also includes a rotating antenna and camera as its third and fourth arm. Finally, a simple conceptual model for cooperative object manipulation is considered, and a suitable setup is designed for practical implementation of the two ICs.

Keywords Augmented object control, Cooperative object manipulation, Multiple impedance control, Space robot

Paper type Research paper

Nomenclature

C	= Vector of quadratic nonlinear terms of velocity, where $\widetilde{C}$ defines this term in task space
G	= Grasp matrix
H	= Positive definite mass matrix of system, where $\widetilde{H}$ defines this term in task space
I	= Second moment of area
$\mathcal{J}_c$	= Jacobian matrix for the manipulators
K_p, K_d, M_{des}	= Gain matrix of controller for object
$\widetilde{K}_p$, $\widetilde{K}_d$, $\widetilde{M}_{des}$	= Gain matrix of controller for system in task space
M_{sys}	= Total mass of rigid subsystem
n	= Number of manipulators
q	= Entity vector of generalized coordinates of rigid system
Q	= Vector of generalized forces

The current issue and full text archive of this journal is available on Emerald Insight at: **www.emeraldinsight.com/0143-991X.htm**

Industrial Robot: An International Journal
44/2 (2017) 198–209

[DOI 10.1108/IR-08-2016-0216]

This work was partially supported by the RoDyMan project, which has received funding from the European Research Council FP7 Ideas under Advanced Grant 320992.

Received 17 August 2016
Revised 19 November 2016
Accepted 21 November 2016

$\widetilde{Q}_{app}$ = Vector of applied control forces
$\widetilde{Q}_{m}$ = Vector of control forces for end-effector motion
$\widetilde{Q}_{react}$ = Vector of forces in task space that are exerted from object to end-effectors
R_{C_0}, $\dot{R}_{C_0}$, $\ddot{R}_{C_0}$ = Vector of position, velocity and acceleration of robot base's in inertial frame
W = Task weighting matrix
$X_E^{(m)}$, $\dot{X}_E^{(m)}$ = Vector of position and velocity of (m)-th end-effectors
$\widetilde{X}^{(m)}$, $\dot{\widetilde{X}}^{(m)}$ = Vector of position and velocity of (m)-th end-effectors in task space
β_0 = Generalized Euler angles variables of the robot base
θ = Generalized variables of the robot joints
θ_o = Object orientation angle
ω = Angular velocity

1. Introduction

Robotic manipulators are widely used in unsafe, costly and repetitive boring tasks (Moosavian *et al.*, 2008; Zarafshan *et al.*, 2016). Actually, mobile manipulator systems can be used in many industrial and service applications, including assembly, inspection and work in hazardous environments. They can interact with an environment or manipulate an object to successfully perform an assumed task. To this end, the control problem of these manipulators during a defined task becomes more challenging. A hybrid position/force control can be used to control interaction forces and system response during contact and object manipulation (Alipour *et al.*, 2015; Navarro-Alarcon *et al.*, 2016; Alipour *et al.*, 2012). However, because of the fact that separate force and position subspaces must be maintained and control mode switching must be made at many points during most tasks, hybrid control does not provide an effective method (Moosavian *et al.*, 2005; Siciliano and Villani, 1999). In fact, mechanical coupling is required for the manipulator to manipulate the object, and, thus, the manipulator may not be treated as an isolated system. To this end, for the manipulator in dynamic interaction with its environment, impedance control (IC) has been proposed, which provides compliant behavior of the manipulator (Rastegari *et al.*, 2006). IC imposes a relation between the force and displacement at the contact point with the environment. Also, IC is a popular method of controlling the dynamic response which a robot has to external forces. The merit of this control strategy is the ability to manipulate in constrained and unconstrained environments. Unlike hybrid control methods that attempt to control forces and motions in orthogonal directions, IC consists of a single control scheme that accommodates both unconstrained and constrained maneuvers. In addition, it is shown that as manipulation is fundamentally a nonlinear problem, the distinction between impedance and admittance is essential, and, because the environment contains inertial objects, the manipulator must be an impedance (Hogan, 1985). Also, it is shown that components of the manipulator impedance may be combined by superposition even when they are nonlinear.

Nevertheless, other control methods exist to perform a successful object manipulation task. In Sitti and Hashimoto (1999), a teleoperated nanoscale object manipulation system was proposed, and its requirements were defined. The system consists of a user interface utilizing a visual and haptic device with a virtual impedance-based bilateral teleoperation control scheme. Also, a novel virtual object frame based on the robot hand configuration was considered in (Wimboeck *et al.*, 2006; Jin *et al.*, 2015; Reis *et al.*, 2015; Wang *et al.*, 2015). The control law takes a desired object frame and desired grasping forces as input which has an intuitive physical meaning. Moreover, stability is obtained even in case a finger loses contact with the object. In Albu-Schaffer *et al.* (2007) and Ott *et al.* (2008), a novel type of ICs for flexible joint robots was proposed. As a target impedance, a desired stiffness and damping was considered without inertia shaping. In addition, lightweight robots were presented which verified the developed controllers and showed the efficiency of the proposed control approach. Also, in Borst *et al.* (2003), an overview over the experiments performed with the DLR hands was presented, and the open problems about hands abilities were clarified. In Tsuji and Kaneko (1999), an IC method was studied which could regulate a virtual impedance between a robot manipulator and external objects using the visual information. They concluded that the conventional IC method was not useful in some cases, where no interaction force between the arm and its environment exists, although it was one of the most effective control methods for manipulators in contact with the environment. In Salehi and Vossoughi (2008), the general problem of IC for a robotic manipulator with a moving flexible base was addressed. This control concept for the flexible base mobile manipulator was the IC method which was combined with sliding mode control methods. Also, a new formulation of computed torque (CT) control was presented in Koningstein (1990), which led to a CT robot controller program. This automated tool was used for simulations and experimental demonstrations of endpoint and object control from a free-flying robot, whereas the shortcoming of improper target impedance selection was presented through analysis and experimentation. A new approach to adapting the target impedance, based upon an on-line estimate of the environment impedance, was proposed and demonstrated. Rehabilitation object manipulation task was presented in Carignan and Olsson (2004). In fact, each haptic master exerts "forces" on a virtual object which, in response, generates desired velocities for the master arm to track. In Lippiello *et al.* (2007), an approach to interaction control of a robot manipulator with a partially known environment was proposed. This algorithm for the online estimation of the object pose was adopted based on the visual data provided by a camera as well as on forces and moments measured during the interaction with the environment. This algorithm was embedded into an IC scheme, resulting in a position-based visual IC. In Zhu and de Schutter (1999), a delicate experiment with control of two heavy-duty industrial robots rigidly holding a raw egg was reported. This experiment indicated that the robots have the capability to perform very delicate operations with the aid of such IC algorithms and force feedback. In the same way, the human characteristics of two humans in a cooperative task (i.e. moving an object by two

humans) were investigated in Rahman *et al.* (2002) using IC strategies. In Meer and Rocky (1995), the stability of the flexible object impedance control (OIC) when coupled to an arbitrary passive environment was studied. Also, the development of a robotic arm with the minimal impedance was presented in Desai and Howe (2001). A good model of the robotic system was developed in this reference so that low gains were used which in turn will lead to low impedance and hence low contact forces in manipulation tasks in unstructured environments. In Meerf and Rocky (1994), a control strategy for the manipulation of flexible objects by multiple robot arms was presented. The control policy developed for flexible objects was based on a controller developed previously for rigid objects: the OIC. For a class of flexible objects, the required extensions to OIC were outlined in this reference. Also, experimental results for a dual-arm robotic system manipulating an object with a single flexible degree of freedom in both free space, and environmental contact tasks were presented therein. In fact, the OIC algorithm enforces the designated impedance not for an individual manipulator endpoint but for the manipulated object itself (Moosavian *et al.*, 2005). The OIC algorithm compensates for the dynamics of both the arms and objects and responds to environmental forces with a fully programmable impedance relationship. In addition, it has been realized that applying the OIC to manipulation of a flexible object may lead to instability (Meer and Rocky, 1995). Based on the analysis of a representative system, it was suggested that to solve the instability problem, one should either increase the desired mass parameters or filter and lower the frequency content of the estimated contact force. Therefore, this leads to the OIC extension law which is considered as Augmented Object Model (AOM) control (Chang *et al.*, 2000). Besides, these two last manipulation algorithms (i.e. OIC and AOM algorithms) are only focused on the manipulated object and do not control the robot base and its manipulators. This can be considered as a weakness of these algorithms which will be fully analyzed in the following. In return, the multiple impedance control (MIC) has been developed for several cooperating manipulators (Moosavian *et al.*, 2005). The MIC enforces the reference impedance on both the manipulator endpoints and the manipulated object. This means that both manipulator end-effectors and the object are controlled to behave like the designated impedance in reaction to any disturbing external force on the object. This is the strength of this algorithm in comparison with the stated impedance algorithms, as will be proven in the paper. Also, to improve the performance of the MIC in dealing with problems such as stability or flexibility, this algorithm is extended and named as non-model based impedance control (Moosavian *et al.*, 2008; Zarafshan *et al.*, 2016).

So, it could be stated that the most important and basic algorithms for the cooperative object manipulation task by a mobile robot are the AOM and MIC algorithms which are found based on the IC, where the former is designed based on the object movement and the latter is designed based on the whole robot movement. Therefore, the comparison of these two aspects or these two algorithms (i.e. AOM and MIC algorithms) is the foundation of this paper. Furthermore, a comprehensive comparison study for these two cooperative object manipulation control strategies is performed in this paper, namely, the AOM control which is focused on the object movement and the MIC algorithm which is concentrated on the movement of both the manipulator end-points and the manipulated object. A case study is considered to analyze the controller performance where a space free-flying robot (SFFR) manipulating an object is simulated. Finally, the two cooperative object manipulation control algorithms are implemented on a simple experimental setup, and the performance of each controller is critically discussed.

2. Augmented object model control

Considering a mobile multi-arm robotic system, the closed-form dynamic model of the system can be obtained as:

$$H^{(i)}(q^{(i)})\,\ddot{q}^{(i)} + C^{(i)}(q^{(i)},\,\dot{q}^{(i)}) + G^{(i)}(q^{(i)}) = Q^{(i)} \tag{1}$$

where $G^{(i)}$ and $Q^{(i)}$ are the vector of the gravity terms and the generalized forces, respectively. Also, the mass matrix is $H^{(i)}$ and the vector of centrifugal and Coriolis terms are $C^{(i)}$ and (i) which indicates the (i)–th manipulator. In the AOM control, the impedance law is considered only to control the object. Thus, the state variables of the controlled object or X_o are used for the IC method (Chang *et al.*, 2000), and the object motion is described by:

$$M\ddot{X}_o = GF_e + F_o + F_c \tag{2}$$

where F_c is the force applied on the object because of contact with the environment, F_e is the applied forces on the object by the robot end-effectors, F_o is the vector of other external forces applied on the object and M is the mass matrix of the object. It follows that the dynamics of the controlled object, and the robots can be expressed using the object state variables as:

$$M_{\oplus}\ddot{X}_{\mathrm{o}} + F_{\oplus} = GF_{\mathrm{e}\oplus} \tag{3}$$

where $M_{\oplus}$ is the mapped inertia matrix, $F_{\oplus}$ is the mapped vector of quadratic velocity terms in the object coordinates, $F_{e\oplus}$ is the total generalized forces that acts on the object by the robot end-effectors and G is the grasping matrix. If the relation between the robot end-effectors in task space $\dot{\tilde{X}}^{(i)}$ and the controlled object coordinates $\dot{X}_o$ is:

$$\dot{\tilde{X}}^{(i)} = R^{obj}_{e(i)}\dot{X}_o \tag{4}$$

then, by considering the equation of motion of the robotic system in equation (1), the mass and nonlinear parameters of the AOM are attained as:

$$\begin{aligned} M_{\oplus} &= M + \sum_{i=1}^{n} R^{obj^T}_{e(i)} H^{(i)} R^{obj}_{e(i)} \\ \mathrm{F}_{\oplus} &= F + \sum_{i=1}^{n} R^{obj^T}_{e(i)} C^{(i)} + \sum_{i=1}^{n} R^{obj^T}_{e(i)} G^{(i)} \end{aligned} \tag{5}$$

where $R^{obj}_{e(i)}$ is the transformation matrix from object coordinates to the robot end-effectors coordinates in task

space. Now, an IC law is applied to equation (2). Choosing the impedance law for the object motion as:

$$M_{des}\ddot{e} + K_d\dot{e} + K_p e = -F_c \tag{6}$$

where $e_o = X_{o_{des}} - X_o$ is the tracking error of object variables, and M_{des}, K_d, K_p are the gain matrices for the proposed IC. Therefore, the exerted forces from end-effectors required to move the object can be obtained as:

$$F_{e_{req}} = G^{\#}F_{e\oplus} = G^{\#}\{M_{\oplus}M_{des}^{-1}(M_{des}\ddot{X}_{des} + K_d\dot{e} + K_p e + F_c) + (F_{\oplus})\} \tag{7}$$

in which $G^{\#}$ is the pseudo inverse of the grasp matrix G as:

$$G^{\#} = W^{-1}G^T(GW^{-1}G^T)^{-1} \tag{8}$$

where it is weighted by a task weighting matrix W (Moosavian *et al.*, 2005).

3. Multiple impedance control strategy

MIC applies the reference impedance to all the manipulator end-points, the manipulated object and the assumed robotic system. This means that all of manipulator end-effectors, the object and the robot base are controlled to behave as the designated impedance (Moosavian *et al.*, 2005). Hence, an accordant motion of the manipulators and payload are achieved. Besides, an object's inertia effects are compensated in the impedance law, and, at the same time, the task space tracking errors are controlled. The applied force commands in the MIC consist of two separate parts. The first one is the motion command which determines the necessary forces for task space variables to track the desired path without the object, and the second one is the force command, which compensates the applied force reactions of the manipulated object on the end-effectors. As stated before, to perform a successful object manipulation task and for the object motion as equation (2), the impedance law for the object motion can be stated as:

$$M_{des}\ddot{e}_o + K_d\dot{e}_o + K_p e_o = -F_c \tag{9}$$

where $e_o = X_{o_{des}} - X_o$ is the tracking error of object variables and M_{des}, K_d, K_p are the gain matrices for the proposed IC. Then, the desired exerted forces from end-effectors to move the object are obtained as:

$$F_{e_{req}} = G^{\#}\{MM_{des}^{-1}(M_{des}\ddot{X}_{o_{des}} + K_d\dot{e}_o + K_p e_o + F_c) + F_w + (F_c + F_o)\} \tag{10}$$

where $G^{\#}$ is the pseudo inverse of **G**. Thus, the force that is applied on the object by the (i)-th end-effectors is directly attained from $F_{e_{req}}$ as:

$$\widetilde{Q}_f^{(i)} = F_{e_{req}} \tag{11}$$

Next, to compute the required force for the motion control, the equations of motion of the mobile robotic system in equation (1) can be written in the task space as:

$$\widetilde{H}^{(i)}(q^{(i)})\ddot{\widetilde{X}}^{(i)} + \widetilde{C}^{(i)}(q^{(i)}, \dot{q}^{(i)}) + \widetilde{G}^{(i)}(q^{(i)}) = \widetilde{Q}^{(i)} \tag{12}$$

where (i) indicates the (i)–th manipulator and $\widetilde{X}^{(i)}$ is the output coordinate, and, thus:

$$\begin{aligned}\widetilde{H}^{(i)} &= \mathcal{J}_c^{(i)^{-T}}H^{(i)}\mathcal{J}_c^{(i)^{-1}}\\ \widetilde{C}^{(i)} &= \mathcal{J}_c^{(i)^{-T}}C^{(i)} - \widetilde{H}^{(i)}\dot{\mathcal{J}}_c^{(i)}\dot{q}^{(i)}\\ \widetilde{G}^{(i)} &= \mathcal{J}_c^{(i)^{-T}}G^{(i)}\\ \widetilde{Q}^{(i)} &= \mathcal{J}_c^{(i)^{-T}}Q^{(i)}\end{aligned} \tag{13}$$

where $\mathcal{J}_c^{(i)}$ is the Jacobian matrix for the (i)-th manipulator, and $\widetilde{X}$ can be considered as the generalized workspace variables of the assumed robot. Also, $\widetilde{Q}^{(i)}$ is the vector of generalized forces in the work space. Similarly, the impedance law for each end-effector can be chosen as:

$$\widetilde{M}_{des}\ddot{\tilde{e}}^{(i)} + \widetilde{K}_d\dot{\tilde{e}}^{(i)} + \widetilde{K}_p\tilde{e}^{(i)} = -F_c \tag{14}$$

where $\tilde{e}^{(i)} = \widetilde{X}_{des} - \widetilde{X}^{(i)}$ is the system tracking error for each manipulator and $\widetilde{M}_{des}$, $\widetilde{K}_d$, $\widetilde{K}_p$ are the gain matrices for the proposed IC of the robotic system. Thus, the required force for the motion control of the end-effectors using the MIC is expressed as:

$$\widetilde{Q}_m^{(i)} = \widetilde{H}^{(i)}\widetilde{M}_{des}^{-1}\left[\widetilde{M}_{des}\ddot{\widetilde{X}}_{des}^{(i)} + \widetilde{K}_d\dot{\tilde{e}}^{(i)} + \widetilde{K}_p\tilde{e}^{(i)} + F_c\right] + \widetilde{C}^{(i)} + \widetilde{G}^{(i)} \tag{15}$$

Also, it has been recommended that the same impedance characteristics for the manipulated object and end-effectors shall be chosen as (Moosavian *et al.*, 2010):

$$M_{des} = \widetilde{M}_{des},\ k_d = \tilde{k}_d,\ k_p = \tilde{k}_p \tag{16}$$

Finally, the required forces for the object manipulation to be supplied by actuators are:

$$\widetilde{Q}^{(i)} = \widetilde{Q}_{app}^{(i)} + \widetilde{Q}_{react}^{(i)} = \widetilde{Q}_m^{(i)} + \widetilde{Q}_f^{(i)} + \widetilde{Q}_{react}^{(i)} \tag{17}$$

where $\widetilde{Q}_m^{(i)}$ is the control forces for the end-effector motion, and $\widetilde{Q}_{react}^{(i)}$ is the reaction load on the end-effectors and virtually cancelled by $\widetilde{Q}_f^{(i)}$ as:

$$\widetilde{Q}_{react}^{(i)} = -F_e^{(i)} \tag{18}$$

where $F_e^{(i)}$ is the exerted forces from end-effectors. Next, substituting equations (18), (15) and (11) into equations (17) and then the results into equation (12) yields:

$$\widetilde{H}^{(i)}(q^{(i)})\left\{\ddot{\widetilde{X}}^{(i)} - M_{des}^{-1}\left[M_{des}\ddot{\widetilde{X}}_d^{(i)} + K_d\dot{\tilde{e}}^{(i)} + K_p\tilde{e}^{(i)}\right]\right\} + G^{\#}M\left\{\ddot{X}_o - M_{des}^{-1}\left[M_{des}\ddot{X}_{o_{des}} + K_d\dot{e}_o + K_p e_o\right]\right\} = 0 \tag{19}$$

Because equation (19) must hold for any $\widetilde{H}^{(i)}$ and M, it can be concluded that:

$$\begin{aligned}&\widetilde{H}^{(i)}(q^{(i)})\left\{\ddot{\widetilde{X}}^{(i)} - M_{des}^{-1}\left[M_{des}\ddot{\widetilde{X}}_d^{(i)} + K_d\dot{\tilde{e}}^{(i)} + K_p\tilde{e}^{(i)}\right]\right\} = 0\\ &M\left\{\ddot{X}_o - M_{des}^{-1}\left[M_{des}\ddot{X}_{o_{des}} + K_d\dot{e}_o + K_p e_o\right]\right\} = 0\end{aligned} \tag{20}$$

By noting that $\widetilde{H}^{(i)}$ and M are positive definite mass matrices, it follows that:

$$\begin{aligned} M_{des}\ddot{\tilde{e}}^{(i)} + K_d\dot{\tilde{e}}^{(i)} + K_p\tilde{e}^{(i)} &= 0 \\ M_{des}\ddot{e}_o + K_d\dot{e}_o + K_p e_o &= 0 \end{aligned} \tag{21}$$

which means all participating manipulators and the manipulated object exhibit the same designated impedance behavior. The block diagram of this proposed control algorithm for the cooperative object manipulation is shown in Figure 1. As stated before, the AOM control is only focused on the object movement, whereas the MIC algorithm is concentrated on the movement of both the manipulator endpoints and the manipulated object together. So, the sole needed force for the object manipulation in the AOM control can be obtained from equation (7) or $F_{e_{req}}$ which is based on the augmented model of the whole system. But, in the MIC strategy, all the $\widetilde{Q}_m^{(i)}$, $\widetilde{Q}_f^{(i)}$ and $\widetilde{Q}_{react}^{(i)}$ are considered to move the robot base, the manipulator endpoints and the manipulated object together on the desired path. So, it can be concluded that there is not any control on the movement of robot base using the AOM control which can be influenced the object manipulation task. To show these facts and in the following, both the AOM and the MIC control strategies are tested in simulation for the assumed space robot to perform an object manipulation task on the designated trajectory. Finally, the experimental study is presented for these two cooperative object manipulation strategies, and the advantages of the MIC strategy are evidenced.

4. CASE-I: space free-flying robot

4.1 Dynamics modelling

SFFRs are space systems that include an actuated spacecraft equipped with few manipulators. Differently from fixed-based manipulators, the spacecraft (base) of a SFFR responds to dynamic reaction forces because of the arms' motion. Unlike long reach space manipulators, SFFRs are suggested to be comparable to the human body and an astronaut, and, thus, they are usually investigated under the assumption of rigid elements. The motion equations of a space robot with rigid components which were described by Moosavian *et al.* (2004) can be rewritten as:

$$\begin{aligned} H(\beta_0,\ \theta)\ \ddot{q} + C_1(\beta_0,\ \dot{\beta}_0,\ \theta,\ \dot{\theta})\ \dot{q} \\ + C_2(\beta_0,\ \dot{\beta}_0,\ \theta,\ \dot{\theta}) = Q(\beta_0, \theta) \end{aligned} \tag{22}$$

where Q is the generalized forces. Also, C_1 and C_2 are the vectors of centrifugal and Coriolis terms, respectively, and H is the mass matrix, where the elements of these matrices can be obtained as:

$$\begin{aligned} H_{ij} = M_{sys}\frac{\partial R_{C_0}}{\partial q_i}\times\frac{\partial R_{C_0}}{\partial q_j} + \frac{{}^0\partial\omega_0}{\partial\dot{q}_i}\times I_0\times\frac{{}^0\partial\omega_0}{\partial\dot{q}_j} \\ + \sum_{m=1}^{n}\sum_{k=1}^{N_m}\left(m_k^{(m)}\frac{\partial r_{C_k}^{(m)}}{\partial q_i}\times\frac{\partial r_{C_k}^{(m)}}{\partial q_j} + \frac{{}^k\partial\omega_k^{(m)}}{\partial\dot{q}_i}\times I_k^{(m)}\times\frac{{}^k\partial\omega_k^{(m)}}{\partial\dot{q}_j}\right) \\ + \left(\sum_{m=1}^{n}\sum_{k=1}^{N_m}m_k^{(m)}\frac{\partial r_{C_k}^{(m)}}{\partial q_i}\right)\times\frac{\partial R_{C_0}}{\partial q_j} + \left(\sum_{m=1}^{n}\sum_{k=1}^{N_m}m_k^{(m)}\frac{\partial r_{C_k}^{(m)}}{\partial q_j}\right)\times\frac{\partial R_{C_0}}{\partial q_i} \end{aligned} \tag{23a}$$

$$\begin{aligned} C_{1ij} = M_{sys}\frac{\partial R_{C_0}}{\partial q_i}\times\left(\sum_{s=1}^{N}\frac{\partial^2 R_{C_0}}{\partial q_s\partial q_j}\dot{q}_s\right) + \frac{{}^0\partial\omega_0}{\partial\dot{q}_i}I_0\frac{{}^0\partial\omega_0}{\partial q_j} + \omega_0 I_0\frac{{}^0\partial^2\omega_0}{\partial\dot{q}_i\partial q_j} \\ + \sum_{m=1}^{n}\sum_{k=1}^{N_m}\left(m_k^{(m)}\frac{\partial r_{C_k}^{(m)}}{\partial q_i}\times\left(\sum_{s=1}^{N}\frac{\partial^2 r_{C_k}^{(m)}}{\partial q_s\partial q_j}\dot{q}_s\right)\right. \\ \left. + \frac{{}^k\partial\omega_k^{(m)}}{\partial\dot{q}_i}I_k^{(m)}\frac{{}^k\partial\omega_k^{(m)}}{\partial q_j} + \omega_k^{(m)}I_k^{(m)}\frac{{}^k\partial^2\omega_k^{(m)}}{\partial\dot{q}_i\partial q_j}\right) \\ + \left(\sum_{s=1}^{N}\frac{\partial^2 R_{C_0}}{\partial q_s\partial q_i}\dot{q}_s\right)\times\sum_{m=1}^{n}\sum_{k=1}^{N_m}\left(m_k^{(m)}\frac{\partial r_{C_k}^{(m)}}{\partial q_j}\right) \\ + \frac{\partial R_{C_0}}{\partial q_i}\times\sum_{m=1}^{n}\sum_{k=1}^{N_m}\left(m_k^{(m)}\sum_{s=1}^{N}\frac{\partial^2 r_{C_k}^{(m)}}{\partial q_s\partial q_j}\dot{q}_s\right) \end{aligned} \tag{23b}$$

$$C_{2i} = -\left(\omega_0 I_0\frac{{}^0\partial\omega_0}{\partial q_i} + \sum_{m=1}^{n}\sum_{k=1}^{N_m}\omega_k^{(m)}I_k^{(m)}\frac{{}^k\partial\omega_k^{(m)}}{\partial q_i}\right) \tag{23c}$$

where ω_0 and I_0 are the angular velocity and moment of inertia matrix of the base, respectively, M_{sys} is the total mass of the rigid subsystem, $\omega_k^{(m)}$ is the angular velocity of the k-th link of the (m)-th manipulator, $r_{C_k}^{(m)}$ is the position vector of mass center of this link with mass of $m_k^{(m)}$ and inertia matrix of $I_k^{(m)}$ and R_{C_0} is the inertial position vector of mass center of the

Figure 1 Block diagram of MIC algorithm for cooperative object manipulation

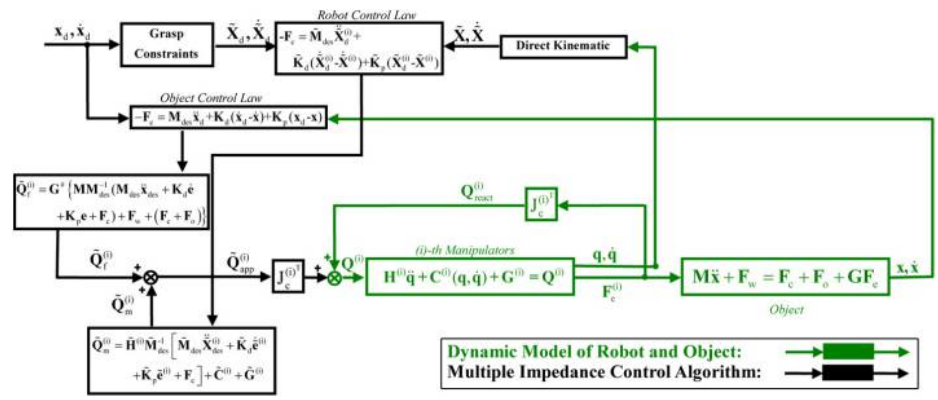

base. The vector q describes the rigid subsystem variable state that is defined as:

$$q = \{R^T, \beta_0^T, \theta^T\}^T \tag{24}$$

where β_0 is a set of Euler angles that determines the orientation of the base, and θ describes joint angles of the links, that is defined as:

$$\theta^T = \left\{\theta_1^{(1)}, \ldots, \theta_{N_1}^{(1)}, \ldots, \theta_1^{(m)}, \ldots, \theta_{N_m}^{(m)}, \ldots, \theta_1^{(n)}, \ldots, \theta_{N_n}^{(n)}\right\}^T \tag{25}$$

where n is the number of manipulators, N_m is the number of links of the (m)-th manipulator and $\theta_{N_m}^{(m)}$ joint angle of the (m)-th of manipulator N_m. Also, Q is the vector of generalized forces and torques that are fully described by Moosavian *et al.* (2004) by determining all dynamics and kinematics parameters. Thus, equation (22) presents the motion's equation of a rigid robot in space, i.e. a microgravity environment.

The assumed robotic system for the simulation study as shown in Figure 2 consists of two 2-degrees of freedom (DOF) planar manipulators and a rotating antenna and a camera as its third and fourth arms, appended with two solar panels. So, the following constraint is considered to grasp the object:

$$(X_A - X_B)^2 + (Y_A - Y_B)^2 = l^2 \tag{26}$$

where X_A and Y_A are the end-effectors' position of the left manipulator, X_B and Y_B are the end-effectors' position of the right manipulator and l is the object length which are fully described in Figure 3. Considering the formulation of MIC, the end-effectors forces are:

$$F_e = \{F_A^x \;\; F_A^y \;\; F_B^x \;\; F_B^y\}^T \tag{27}$$

Therefore, the equations of motion for the grasped object are:

$$\begin{cases} F_A^x + F_B^x = m\ddot{X}_o \\ F_A^y + F_B^y = m\ddot{Y}_o \\ (F_B^x - F_A^x)l/2C_0 + (F_B^y - F_A^y)l/2S_0 = I\ddot{\theta}_o \end{cases} \tag{28}$$

where S_0 and C_0 stand to the sin and cos functions of the object orientation or θ_o, respectively. Thus, the grasp matrix is obtained as:

Figure 2 The considered space robotic system

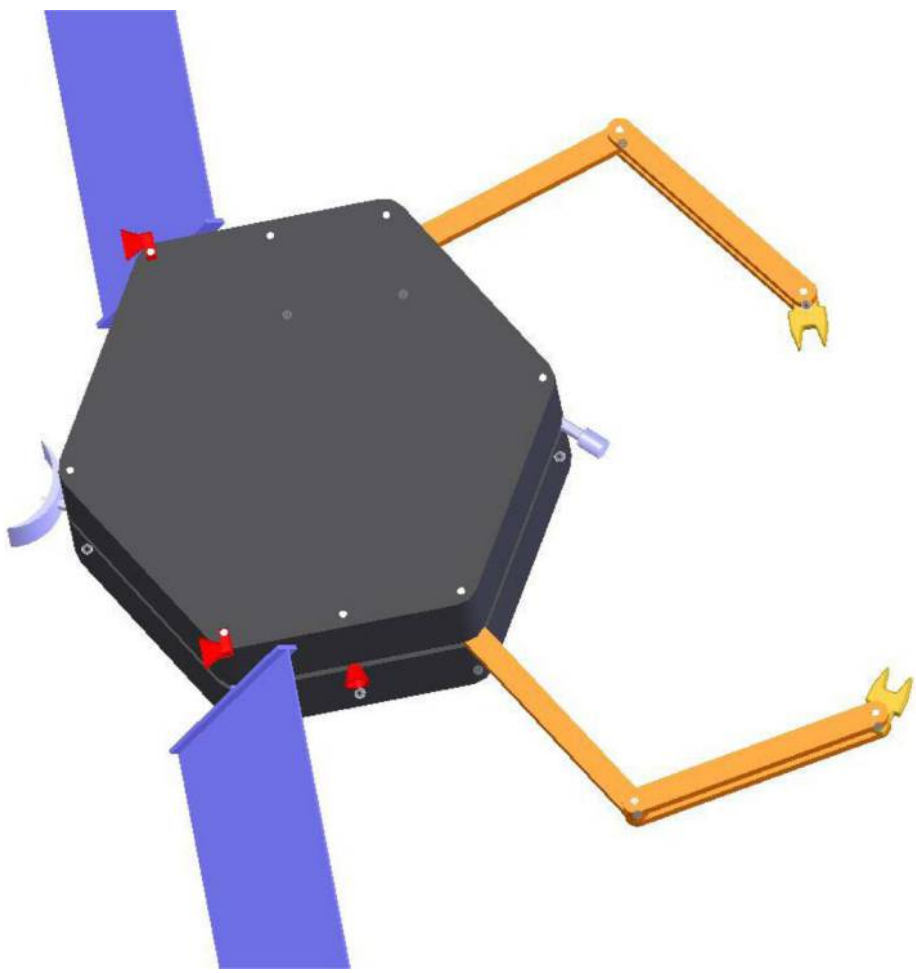

Figure 3 Schematic representation of assumed space robot and its geometric parameters

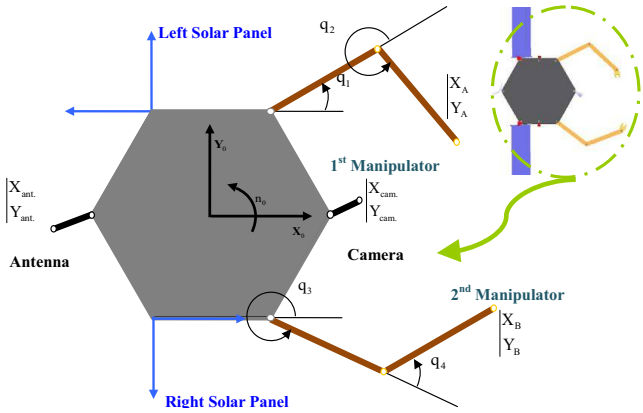

$$G = \begin{bmatrix} 1 & 0 & 1 & 0 \\ 0 & 1 & 0 & 1 \\ -1/2C_0 & -1/2S_0 & 1/2C_0 & 1/2S_0 \end{bmatrix} \quad (29)$$

Moreover, considering the MIC formulation for this robotic system with $\widetilde{X}^{(i)}$ as the output coordinate:

$$\widetilde{X}^{(i)} = \begin{bmatrix} X_{C_0} & Y_{C_0} & d_{C_0} & X_{E,A} & Y_{E,A} & X_{E,B} & Y_{E,B} & d_{Ant} & d_{Cam} \end{bmatrix}^T \quad (30)$$

where for the assumed SFFR in Figure 2, the transformation matrix is:

$$R^{obj}_{e(i)} = \begin{bmatrix} 0 & 0 & 0 & 1 & 0 & 1 & 0 & 0 & 0 \\ 0 & 0 & 0 & 0 & 1 & 0 & 1 & 0 & 0 \\ 0 & 0 & 0 & -0.5lC_0 & -0.5lS_0 & 0.5lC_0 & 0.5lS_0 & 0 & 0 \end{bmatrix}^T \quad (31)$$

Table I The geometric and mass parameters of the assumed SFFR

	i, j		
$i = 1$	$i = 2$		
j	m_{ij} (kg)	l (m)	$I_{z_{ij}}$ (kg.m^2)
0	50	1	10
1	4	1	0.5
2	3	1	0.5

Table II The initial condition of the simulation study and controller gains

$q(0) = [0\ 0\ 0\ 0.6\ 4.2\ 5.6\ 2.1\ \pi/7\ \pi/36]^T$	$\dot{q}(0) = [0.85\ 0\ 0\ 0\ 0\ 0\ 0\ 0\ 0]^T$
$K_p = \widetilde{K}_p = 900$	$K_d = \widetilde{K}_d = 300$

Figure 4 Error of the work space variables during object manipulation for SFFR

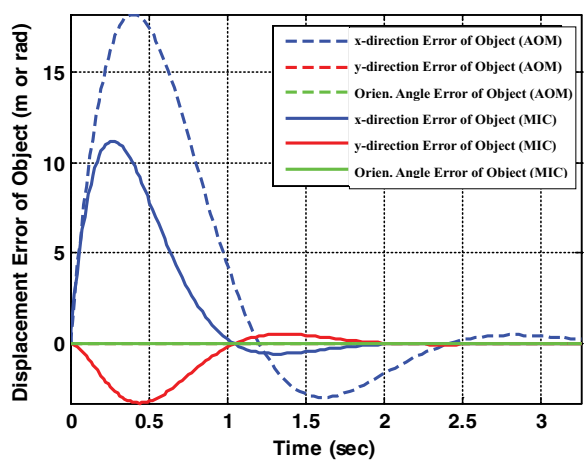

Figure 5 Error of the variable rates during object manipulation for SFFR

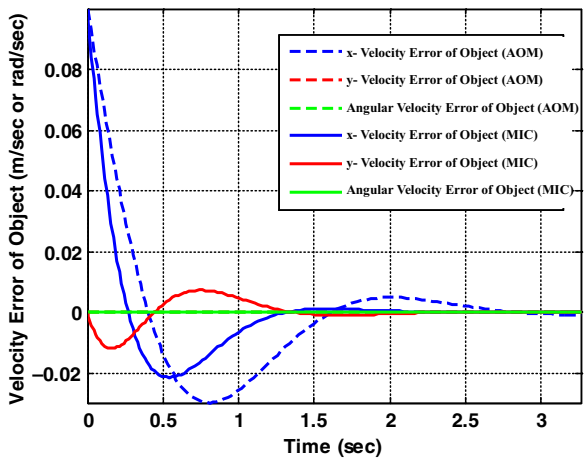

Figure 6 An animated view of the system during cooperative object manipulation

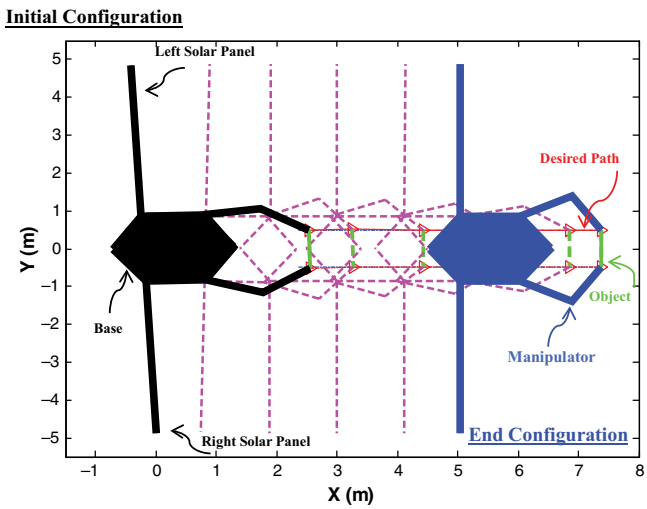

Figure 7 Schematic representation of the conceptual robotic system

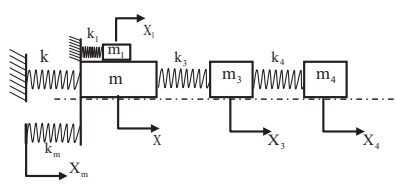

4.2 Simulation results and discussions

Considering the geometric and mass parameters for the assumed SFFR system as given in Table I as they are applied by Moosavian *et al.* (2005), the simulation study is carried out using the initial condition (Table II) for both AOM and MIC strategies. Also, a MATLAB/SIMULINK program is used to simulate and implement the stated control algorithms on the assumed space robot. It should be noted that the extracted dynamic model of the space robot was verified by Zarafshan *et al.* (2013). In addition, a manipulation operation is considered along a straight path. To perform this task by the robot, several solutions exist. The first scenario is that the two manipulators of the robot capture the object and perform this operation by the base movement. The second one is that the base remains stationary and performs the task using its manipulators, whereas the desired path to follow is within the fixed work space of the manipulators. The third scenario is achieved by combining the two. Considering the desired path

Figure 8 3D view of the manufactured setup

length, only the MIC strategy can perfectly control and move the robot based on the considered path using $\widetilde{Q}_m^{(i)}$ term or the motion force which is only considered note in the MIC algorithm versus the AOM strategy. In fact, if the defined generalized variable of the robot base and the end-effectors [the generalized workspace variables of the robot or $\widetilde{X}^{(i)}$ which is defined in equation (30) for this case study] are entirely controlled, the object would be on the desired path which is the basis of the MIC algorithm. So, as shown in Figures 4 and 5, the MIC system can successfully perform the object manipulation task in regarding to the AOM controller. Actually, the MIC method can perfectly control the object on the designed straight path for the manipulation operation. In addition, as shown from these figures, the MIC algorithm has the better performance over the AOM algorithm for the same controller's gains (Table II). This means that even though there is no control of the robot base in the AOM algorithm, the object manipulation task may not perfectly perform when the desired path/trajectory is not within the fixed work space of the assumed robot. Finally, an animated view of the system performing the object manipulation using the MIC strategy along the straight path is shown in Figure 6.

5. CASE-II: experimental study

5.1 Dynamics modelling

In this section, a simple conceptual model (which is proposed by Hogan) for the object manipulation operation is considered to compare various control methods by a single manipulator. This conceptual model is used to study the basic analysis of the operation in most object manipulation algorithms (Figure 7). In this progress, the object manipulation operation is defined based on the object motion by the considered path. According to this model, the setup is designed for the practical implementation (Figure 8), and some object manipulation controllers are tested. Assuming that this vibration system is intended as Figure 7, then the motion equations of the system can be obtained. Hence, if:

$$\begin{array}{l} X > X_1, X_3 \\ X_m > X \\ X_3 > X_4 \end{array} \tag{32}$$

then, it is:

Figure 9 Crank-slider mechanism on the motor input

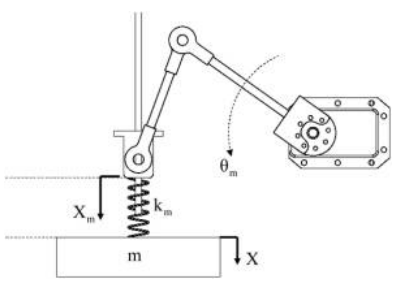

$$\begin{cases} m\ddot{X} = k_m(X_m - X) - k_1(X - X_1) - k_2(X - X_2) - k_3(X - X_3) \\ m_1\ddot{X}_1 = k_1(X - X_1) \\ m_2\ddot{X}_2 = k_2(X - X_2) \\ m_3\ddot{X}_3 = k_3(X - X_3) - k_4(X_3 - X_4) \\ m_4\ddot{X}_4 = k_4(X_3 - X_4) \end{cases} \tag{33}$$

or in vector form:

$$M\ddot{\underline{X}} + K\underline{X} = Bu \tag{34}$$

Figure 10 Control block diagram, sensors, electrical components and motor of the setup

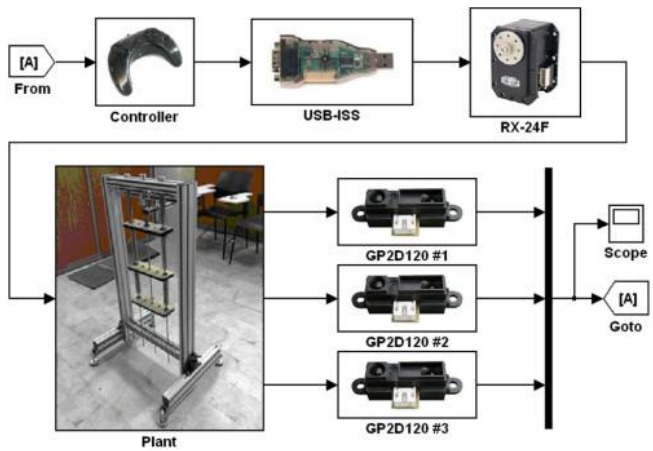

Table III The parameters and mass specifications of the manufactured setup

m = 400 (gr)	K = 70 (N/m)
m_3 = 400 (gr)	K_3 = 70 (N/m)
m_4 = 175 (gr)	K_4 = 57 (N/m)

Figure 11 Result comparison of the AOM and MIC implementation on the setup

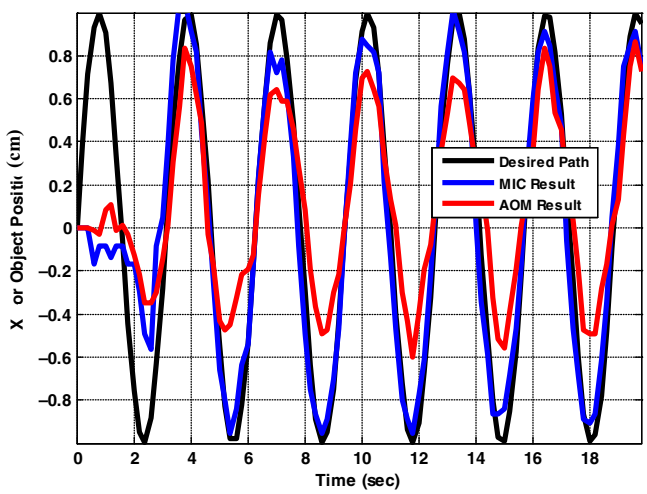

in which X is the state variables of the system, which corresponds to the displacement of each mass as:

$$X = [X \;\; X_1 \;\; X_2 \;\; X_3 \;\; X_4]^T \tag{35}$$

where each of these variables can be defined as generalized variables of a robot, end-effectors, object and other members in the dynamic modelling of the system. Moreover, M is the mass matrix of the system which can be stated as:

$$M = \begin{bmatrix} \mathrm{m} & 0 & 0 & 0 & 0 \\ 0 & m_1 & 0 & 0 & 0 \\ 0 & 0 & m_2 & 0 & 0 \\ 0 & 0 & 0 & m_3 & 0 \\ 0 & 0 & 0 & 0 & m_4 \end{bmatrix} \tag{36}$$

and K is the stiffness matrix of the system as:

$$K = k\begin{bmatrix} k_{\mathrm{m}} + k_1 + k_2 + k_3 & -k_1 & -k_2 & -k_3 & 0 \\ -k_1 & k_1 & 0 & 0 & 0 \\ -k_2 & 0 & k_2 & 0 & 0 \\ -k_3 & 0 & 0 & k_3 + k_4 & -k_4 \\ 0 & 0 & 0 & -k_4 & k_4 \end{bmatrix} \tag{37}$$

where k_m is the spring stiffness which is mounted on the slider output. The crank-slider mechanism and its spring which can be named as the input mechanism are mounted on the motor input. This causes the system has its degrees of freedom even if the motor is stopped (Figure 9). Therefore, the input forces to the system are related to the slider position and its spring stiffness or k_m. Also, u is the system input or the motor displacement X_m and B matrix is equal to:

$$B = [k_m \;\; 0 \;\; 0 \;\; 0 \;\; 0]^T \tag{38}$$

Figure 12 Position of input mechanism considering control input

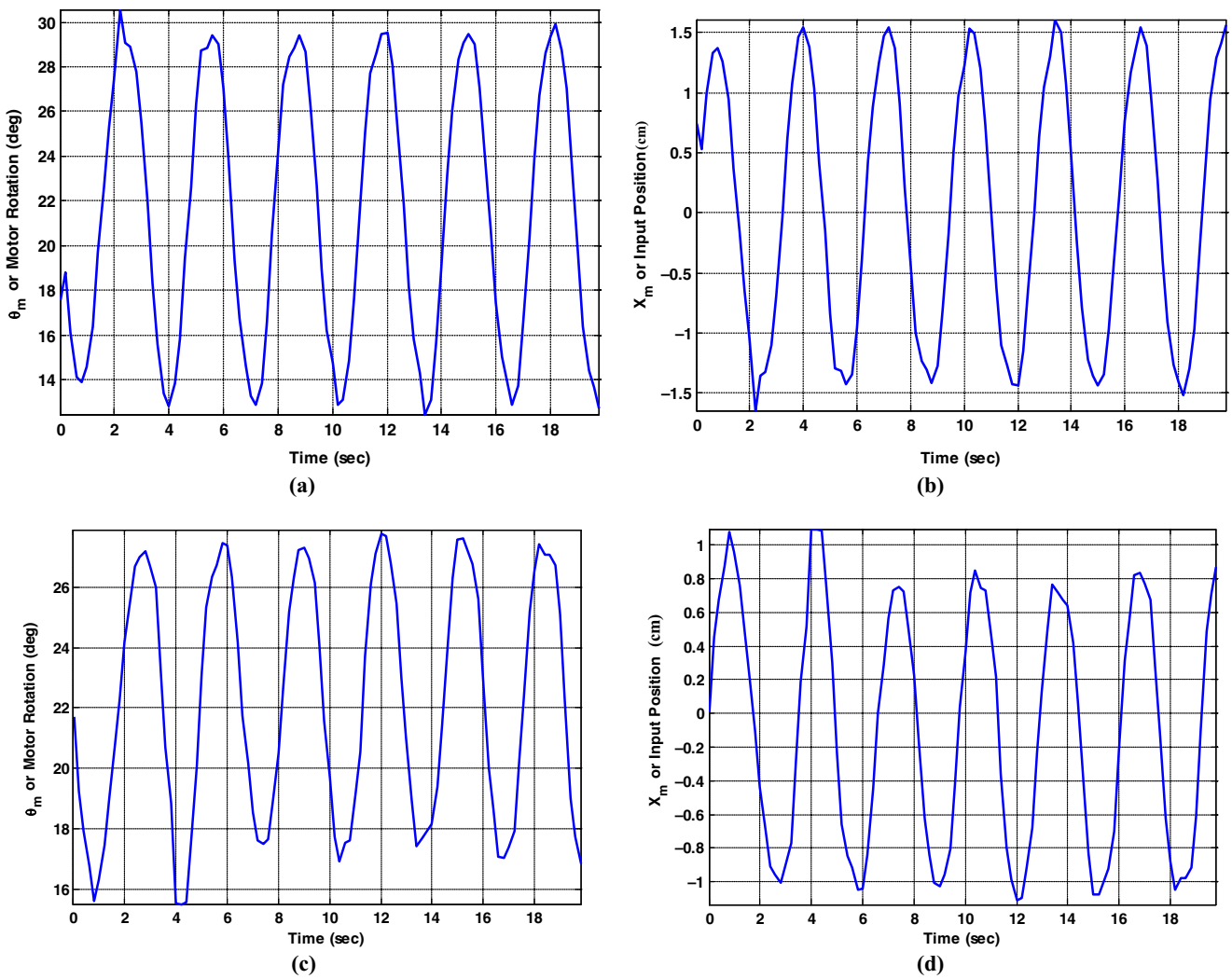

Notes: (a) Motor rotation (θ_m) for MIC; (b) Slider position (X_m) for MIC; (c) Motor rotation (θ_m) for AOM; (d) Slider position (X_m) for AOM

Given this system, the motion of the fourth body or X_4 should be adapted to the designed path. Also, it is imposed by the force of input mechanism. It should be noted that damping components are not installed on this system. Moreover, the input force is obtained by changing the spring length which is installed on the output of the crank-slider mechanism. In the same way, the details of this manufactured control test bed are studied here. This conceptual robotic system has 5 DOF and includes the frame, electrical motor, mass, springs and sensors as shown in Figure 8. Also, Figure 10 represents the system software which is designed in MATLAB/Simulink program. As shown in this figure, the sensor outputs are compared with the desired input, and, then, this difference is exerted to the controller in each loop to obtain the controller output based on the assumed control law. This controller output is applied to the electrical motor (RX-24F) using an A/D converter (USB-ISS). Therefore, this motor moves the first mass using the crank-slider mechanism. This causes the total system to move, and, then, the desired output for the fourth mass is attained. At last, all of these displacements are sensed and fed back by the position sensors (Sharp Sensors, GP2D120) which are installed for each mass. This process completes the closed-loop control algorithm in each time step. Also, the parameters and mass specifications of this setup are stated in Table III.

5.2 Experimental results and discussion

Both the MIC and AOM algorithms are applied on this setup to control the position of the fourth mass (X_4) on the designed path\trajectory (in this case study, $X_{des} = Sin(t)$). This variable is considered as the object position. Also, the results for this implementation are represented in Figure 11. As shown in this figure, a successful object manipulation operation is performed by controlling the position of the first mass or the robot base (X) and the position of the third mass or the robot manipulator (X_3) together. This is achieved when the MIC algorithm is applied. The position of the slider and the motor rotation at the time of this operation are shown in Figure 12(a) and (b). In the same way, as shown in Figure 11, perfect object manipulation task is not obtained by applying the AOM algorithm on the system which only controls the position of the fourth mass (X_4). This is explained by observing that this control approach is found on the control of the object position (position of the fourth mass or X_4). Actually, this fact is the main weakness of this strategy versus the MIC strategy. As shown in Figure 11, this superiority in the controller performance is well captured by this study. For the sake of completeness, the position of the slider and the motor rotation for this operation using the AOM algorithm are shown in Figure 12(c) and (d).

6. Conclusions

As concluded from the introduction, it could be stated that the most important and basic algorithms for the cooperative object manipulation task by a mobile robot are the AOM and MIC algorithms which were found based on the IC. So, in this paper, a comprehensive comparison study for these usual cooperative object manipulation control strategies was performed. In fact, the former is focused only on the object movement, whereas the latter is concentrated on the movement of the robot base, the manipulator endpoints and the manipulated object. Thus, the basis of these two algorithms was fully studied. To this end, a case study has been simulated in which a SFFR system is used to manipulate an object using the above control strategies. Next, these two object manipulation control algorithms were implemented on a conceptual model which was considered to study the basic analysis of the operation in object manipulation algorithms. The results revealed that the MIC system could successfully perform the object manipulation task, as opposed to the AOM controller: for the same controller gains, the MIC strategy showed better performance than the AOM strategy. This means that because there is no control on the robot base with the AOM algorithm, the object manipulation task cannot be satisfactorily performed whenever the desired path is not within the robot work space. On the other hand, with the MIC algorithm satisfactory object manipulation is achieved for a mobile robotic system in which the robot base, the manipulator endpoints and the manipulated object shall be moved.

References

Albu-Schaffer, A., Ott, C.H. and Hirzinger, G. (2007), "A unified passivity based control framework for position, torque and impedance control of flexible joint robots", *International Journal of Robotics Research*, Vol. 26 No. 1, pp. 23-39.

Alipour, K., Moosavian, S. and Ali, A. (2012), "Effect of terrain traction, suspension stiffness and grasp posture on the tip-over stability of wheeled robots with multiple arms", *Journal of Advanced Robotics*, Vol. 26 Nos 8/9, pp. 817-842.

Alipour, K., Moosavian, S. and Ali, A. (2015), "Dynamically stable motion planning of wheeled robots for heavy object manipulation", *Journal of Advanced Robotics*, Vol. 29 No. 8, pp. 545-560.

Borst, C.H., Fischer, M., Haidacher, S., Liu, H. and Hirzinger, G. (2003), "DLR hand II: experiments and experiences with an anthropomorphic hand", *IEEE International Conference on Robotics & Automation*, *Taipei*, pp. 702-707.

Carignan, C.R. and Olsson, P.A. (2004), "Cooperative control of virtual objects over the internet using force-reflecting master arms", *IEEE International Conference on Robotics and Automation*, *New Orleans, LA*, pp. 1221-1226.

Chang, K., Holmberg, R. and Khatib, O. (2000), "The augmented object model: cooperative manipulation and parallel mechanism dynamics", *IEEE International Conference on Robotics and Automation*, *San Francisco, CA*, pp. 470-475.

Desai, J.P. and Howe, R.D. (2001), "Towards the development of a humanoid arm by minimizing interaction forces through minimum impedance control", *IEEE International Conference on Robotics and Automation*, *Seoul*, pp. 4214-4219.

Hogan, N. (1985), "Impedance control: an approach to manipulation: part 1-theory", *Journal of Dynamic Systems, Measurement, and Control*, Vol. 107 No. 1.

Jin, H., Zhang, L., Rockel, S., Zhang, J., Hu, Y. and Zhang, J. (2015), "A novel optical tracking based tele-control system

for tabletop object manipulation tasks", *IEEE/RSJ International Conference on Intelligent Robots and Systems (IROS)*, *Hamburg*, pp. 636-642.

Koningstein, R. (1990), "Experiments in cooperative-arm object manipulation with a two-armed free-flying robot", PhD thesis, Aerospace Robotics Laboratory, Department of Aeronautics and Astronautics Stanford University.

Lippiello, V., Siciliano, B. and Villani, L. (2007), "Position-based visual servoing in industrial multi-robot cells using a hybrid camera configuration", *IEEE Transactions on Robotics*, Vol. 23, pp. 73-86.

Meer, D.W. and Rocky, S.M. (1995), "Coupled-system stability of flexible-object impedance control", *IEEE International Conference on Robotics and Automation*, *Nagoya*, pp. 1839-1845.

Meerf, D.W. and Rocky, S.M. (1994), "Experiments in object impedance control for flexible objects", *IEEE International Conference on Robotics and Automation*, *San Diego, CA*, pp. 1222-1227.

Moosavian, S., Ali, A. and Ashtiani, H.R. (2008), "Cooperation of robotic manipulators using non-model-based multiple impedance control", *Journal of Industrial Robot*, Vol. 35 No. 6, pp. 549-558.

Moosavian, S., Ali, A. and Pourreza, A. (2010), "Heavy object manipulation by a hybrid serial-parallel mobile robot", *International Journal of Robotics and Automation*, Vol. 25 No. 2, p. 109.

Moosavian, S., Ali, A. and Papadopoulos, E. (2004), "Explicit dynamics of space free-flyers with multiple manipulators via SPACEMAPLE", *Journal of Advanced Robotics*, Vol. 18 No. 2, pp. 223-244.

Moosavian, S., Ali, A., Rastegari, R. and Papadopoulos, E. (2005), "Multiple impedance control for space free-flying robots", *AIAA Journal of Guidance, Control, and Dynamics*, Vol. 28 No. 5, pp. 939-947.

Navarro-Alarcon, D., Yip, H.M., Wang, Z., Liu, Y., Zhong, F., Zhang, T. and Li, P. (2016), "Automatic 3-D manipulation of soft objects by robotic arms with an adaptive deformation model", *IEEE Transactions on Robotics*, Vol. 32 No. 2, pp. 429-441.

Ott, C.H., Albu-Schaffer, A., Kugi, A. and Hirzinger, G. (2008), "On the passivity-based impedance control of flexible joint robots", *IEEE Transactions on Robotics*, Vol. 24 No. 2, pp. 416-429.

Rahman, M.D.M., Ikeura, R. and Mizutani, K. (2002), "Cooperation characteristic if two humans in moving an object", *Machine Intelligence and Robotic Control*, Vol. 4 No. 2, pp. 43-48.

Rastegari, R., Moosavian, S. and Ali, A. (2006), "Multiple impedance control of space free-flying robots using virtual object grasp", *IEEE/RSJ International Conference on Intelligent Robots and Systems*, *Beijing*, pp. 3125-3130.

Reis, F.M., Leite, A.C., From, P.J., Hsu, L. and Lizzaralde, F. (2015), "Visual servoing for object manipulation with multifingered robot hand", *IFAC Paper Online*, Vol. 48 No. 19, pp. 1-6.

Salehi, M. and Vossoughi, G.H. (2008), "Impedance control of flexible base mobile manipulator using singular perturbation method and sliding mode control law", *International Journal of Control, Automation, and Systems*, Vol. 6 No. 5, pp. 677-688.

Siciliano, B. and Villani, L. (1999), *Robot Force Control*, Kluwer Academic Publishers, Boston, MA.

Sitti, M. and Hashimoto, H. (1999), "Teleoperated nano scale object manipulation", *Recent Advances on Mechatronics*, Springer.

Tsuji, T. and Kaneko, M. (1999), "Noncontact impedance control for redundant manipulators", *IEEE Transactions on Systems, Man, and Cybernetics – Part A: Systems and Humans*, Vol. 29 No. 2, pp. 184-193.

Wang, Y., Ewert, D., Vossen, R. and Jeschke, S. (2015), "A visual servoing system for interactive human-robot object transfer", *Journal of Automation and Control Engineering*, Vol. 3 No. 4, pp. 277-283.

Wimboeck, T., Ott, C.H. and Hirzinger, G. (2006), "Passivity-based object-level impedance control for a multi-fingered hand", *IEEE/RSJ International Conference on Intelligent Robots and Systems*, *Beijing*, pp. 4621-4627.

Zarafshan, P., Moosavian, S. and Ali, A. (2013), "Dynamics modelling and hybrid suppression control of space robots performing cooperative object manipulation", *Journal of Communications in Nonlinear Science and Numerical Simulation*, Vol. 18, pp. 2807-2824.

Zarafshan, P., Moosavian, S., Ali, A. and Papadopoulos, E.G. (2016), "Adaptive hybrid suppression control to perform cooperative object manipulation in space", *Robotica*, Vol. 34 No. 7, pp. 1464-1485.

Zhu, W. and de Schutter, J. (1999), "Control of two industrial manipulator rigidly holding an egg", *IEEE Control Systems*, Vol. 19 No. 2, pp. 24-30.

Corresponding author

Payam Zarafshan can be contacted at: p.zarafshan@ut.ac.ir